

Experimental demonstration of quantum walks with initial superposition states

Qi-Ping Su¹, Yu Zhang¹, Li Yu¹, Jia-Qi Zhou¹, Jin-Shuang Jin¹, Xiao-Qiang Xu¹, Shao-Jie Xiong^{1,3}, QingJun Xu¹, Zhe Sun¹, Kefei Chen², Franco Nori^{4,5*} and Chui-Ping Yang^{1*}

¹*Department of Physics, Hangzhou Normal University, Hangzhou, Zhejiang 310036, China*

²*Department of Mathematics, Hangzhou Normal University, Hangzhou 310036, China*

³*State Key Laboratory of Precision Spectroscopy, Department of Physics, East China Normal University, Shanghai 200062, China*

⁴*Theoretical Quantum Physics Laboratory, RIKEN Cluster for Pioneering Research, Wako-shi, Saitama 351-0198, Japan and*

⁵*Department of Physics, University of Michigan, Ann Arbor, Michigan 48109-1040, USA*

(Dated: May 1, 2019)

The preparation of initial superposition states of discrete-time quantum walks (DTQWs) are necessary for the study and applications of DTQWs. In linear optics, it is easy to prepare initial superposition states of the coin, which are always encoded by polarization states; while the preparation of superposition states of the walker is challenging. Based on a novel encoding method, we here propose a DTQW protocol in linear optics which enables the preparation of arbitrary initial superposition states of the walker and the coin. With this protocol, we report an experimental demonstration of DTQW with the walker initially in superposition states, by using only passive linear-optical elements. The effects of the walker's different initial superposition states on the spread speed of the DTQW and on the entanglement between the coin and the walker are also experimentally investigated, which have not been reported before. When the walker starts with superposition states, we show that the properties of DTQW are very different from those of DTQW starting with a single position. Our findings reveal different properties of DTQW and paves an avenue to study DTQW with arbitrary initial states. Moreover, the encoding method enables one to encode an arbitrary high-dimensional quantum state using a single physical qubit and may be adopted to implement other quantum information tasks.

arXiv:1805.09784v3 [quant-ph] 30 Apr 2019

* Email: yangcp@hznu.edu.cn, Telephone number: +86-571-28860503 office, +86-571-28865286 fax; andEmail: fnori@riken.jp, Telephone number: +8

I. INTRODUCTION

Quantum walks (QWs) are extensions of the classical random walk [1] and have wide applications in quantum algorithms [2–4], quantum simulations [5–10], quantum computation [11–13], and so on [14, 15]. In standard one-dimensional (1D) discrete-time quantum walks (DTQWs) [16, 17], the walker’s position can be denoted as $|x\rangle$ (x is an integer) and the coin can be described with the basis states $|0\rangle_c$ and $|1\rangle_c$. The evolutions of the walker and the coin are usually characterized by a time-independent unitary operator $U = TS_c(\psi)$. In each step, the coin is tossed by

$$S_c(\psi) = \begin{pmatrix} \cos \psi & -\sin \psi \\ \sin \psi & \cos \psi \end{pmatrix}$$

with $\psi \in (0^\circ, 90^\circ)$, and the walker is shifted by $T = \sum_x |x+1\rangle\langle x| \otimes |1\rangle_c\langle 1| + \sum_x |x-1\rangle\langle x| \otimes |0\rangle_c\langle 0|$. In general, the result of the DTQW with a finite number of steps is determined by the initial states of the coin and the walker as well as the operator U . The systematic investigation of DTQW properties and the effect of the initial states on DTQW is important and necessary for applications of DTQW.

It is worth noting that DTQW with the walker initially in a superposition state has not been demonstrated in experiments, though there were several theoretical works [18–22]. DTQWs have been experimentally realized in several systems, such as linear optics [4–6, 23–25], ion traps [27, 28], cavity quantum electrodynamics [29], and neutral atom traps [30]. In these DTQW experiments, the walker always starts from the original position $|0\rangle$. In most DTQW experiments, it is difficult to prepare an arbitrary initial quantum superposition states of the walker. Moreover, initial superposition states of the walker are usually required for applications of DTQW. For example, an initial uniform superposition state of the walker’s position is required in the Grover walk [2]. The DTQW with initial superposition states of the walker are quite different from the standard DTQW (i.e., the walker starts from a single position $|x\rangle$), because the final state of the former is a coherent superposition of the final states of the standard DTQW starting from different single positions and thus contains more quantum interference.

Note that the effects of the coin’s initial state on DTQW have been well studied [16, 17, 23–26] but the effects of the walker’s initial superposition states on DTQW have not been investigated before in linear optics. In previous linear-optical DTQW implementations [31–33], the coin was always encoded in the 2-dimensional polarization space and the position of the walker must be encoded in high-dimensional spaces. In [31], the coin was encoded using the polarization state and the walker’s positions were encoded using the paths of the photons, in which an additional calcite beam displacer was needed in each step, to perform the conditional shift of the walker and DTQWs with up to 6 steps were measured in experiments. In [32], the coin was also encoded using the polarization state and the walker’s positions were encoded using the temporal information of single photons, in which the coin operator was adjustable and 5-step DTQWs were studied experimentally. In linear optics, the preparation of arbitrary initial superposition states of the coin is not difficult because it is easy to obtain arbitrary polarization states using half-wave plates (HWPs) and quarter-wave plates (QWPs). However, the preparation of arbitrary initial superposition states of the walker is difficult.

To our knowledge, how to encode the walker’s position using the polarization state has not been reported in both theory and experiment. It is difficult to encode a high-dimensional state using the two-dimensional state. If the walker’s position is encoded using the polarization state, arbitrary initial superposition states of the walker can be easily prepared in linear-optical experiments.

In this work, we propose an encoding method to encode and read out high dimensional states with a two-dimensional qubit. With this method, we report the first DTQW protocol with the walker’s position encoded in the polarization space of single photons. The DTQW protocol together with the design of linear optical setup, in which the coin is encoded by two paths, allows us to arbitrarily set the input state of the walker and coin. Since the DTQW with initial superposition states of coin has been well studied, here we focus on the experimental implementation of DTQW with the walker initially in superposition states, which has not been reported before. In this case, the effect of the walker’s different initial superposition states on the spread speed of the walker and on the entanglement between the coin and the walker (i.e., the entropy of the reduced density matrix of the coin) are studied experimentally.

II. RESULTS

DTQW Protocol in Linear Optics

To implement DTQW in polarization space, we propose a novel encoding method in the Method section. Here we make the specific choice of encoding the walker’s positions using non-orthogonal states $|k\rangle_p = \cos \theta_k |H\rangle + e^{i\phi_k} \sin \theta_k |V\rangle$ (with integer k) in the polarization space of single photons, by setting $\theta_k = k\Delta\theta$ and $\phi_k = 0$. The coin is encoded by

two paths $|0\rangle$ and $|1\rangle$ of the single photons. As shown in Fig. 1(a), the operator for the conditional translation of $|k\rangle_p$ should be expressed as

$$T_p = \sum_k |k+1\rangle_p \langle k| \otimes |1\rangle \langle 1| + \sum_k |k-1\rangle_p \langle k| \otimes |0\rangle \langle 0|.$$

In this case, the coin operator S_c can be implemented by a $\cos^2 \psi / \sin^2 \psi$ beam splitter (BS) and the operator T_p can be implemented via two HWPs oriented at 0° and two HWPs oriented at $\Delta\theta/2$ (step forward) and $-\Delta\theta/2$ (step back), as shown in Fig. 1(b). Note that each HWP oriented at 0° can be replaced by a mirror.

In each step of DTQW in polarization space, the state of the system can be expressed as $|\Psi_0\rangle_p |0\rangle + |\Psi_1\rangle_p |1\rangle$, with

$$\begin{aligned} |\Psi_0\rangle_p &= \frac{1}{N_p} \sum_{k=-n}^n a_k |k\rangle_p = \frac{1}{N_a} \sum_{k=-n}^n a'_k |k\rangle_p, \\ |\Psi_1\rangle_p &= \frac{1}{N_p} \sum_{k=-n}^n b_k |k\rangle_p = \frac{1}{N_b} \sum_{k=-n}^n b'_k |k\rangle_p, \end{aligned} \quad (1)$$

where $a'_k = a_k/C_a$, $b'_k = b_k/C_b$, $C_a = \sqrt{\sum_k |a_k|^2}$, $C_b = \sqrt{\sum_k |b_k|^2}$, $N_a = N_p/C_a$, $N_b = N_p/C_b$, and N_p is the normalization coefficient, which guarantees $\sum_k |a_k|^2 + \sum_k |b_k|^2 = 1$. If one derives all values of a_k and b_k , the probability distribution of the DTQW can be obtained as $|a_k|^2 + |b_k|^2$.

The values of a_k (b_k) can be obtained by using $a_k = C_a a'_k$ ($b_k = C_b b'_k$). Note that $|\Psi_0\rangle_p$ ($|\Psi_1\rangle_p$) has the same form as that of $|\Psi\rangle_q$ in the Eq. (4) and the condition $\sum_k |a'_k|^2 = 1$ ($\sum_k |b'_k|^2 = 1$) is satisfied. By using the encoding method introduced in the section II, a'_k and b'_k can be obtained one at a time by implementing the DTQW with different angles $\Delta\theta$ and measuring $|\Psi_0\rangle_p$ and $|\Psi_1\rangle_p$ in path $|0\rangle$ and path $|1\rangle$, respectively. Next, C_a and C_b can be obtained by solving two equations

$$C_a^2 + C_b^2 = 1 \quad \text{and} \quad \frac{C_a^2}{C_b^2} \cdot \frac{|\sum_k a'_k \cos(k\theta)|^2}{|\sum_k b'_k \sin(k\theta)|^2} = r, \quad (2)$$

where $r = |\sum_k a_k \cos(k\theta)|^2 / |\sum_k b_k \sin(k\theta)|^2$ is the ratio between the number of photons counted in path $|0\rangle$ and that counted in path $|1\rangle$ at the same time period for an arbitrary $\theta \neq 0$. With this protocol, DTQW with the walker initially in an arbitrary superposition state can be easily implemented.

Experimental demonstrations

A feasible linear-optical setup for DTQW in the photon polarization space is shown in Fig. 2. A pair of photons are generated by the type-I spontaneous parametric down conversion in a 3-mm-thick nonlinear beta-barium borate (BBO) crystal pumped by a 100 mW diode laser (centered at 405.8 nm). One photon is directly detected by detector D_0 as the trigger and the other photon is adopted to make DTQW. Then an arbitrary coin state can be initialized by a combination of one polarizing beam splitter (PBS), two quarter-wave plates (QWPs), and one HWP. An arbitrary state of the walker's position is represented as a polarization state, which can be easily initialized by using two HWPs on the two paths of the DTQW photon after the PBS.

In Fig. 3, we show the results of the 1D Hadamard (i.e., setting $\psi = \pi/4$) DTQW with an initial state of $(0.8| -1\rangle_p + 0.6|1\rangle_p)|0\rangle$. Besides the probability distribution of the walker's position $|a_k|^2 + |b_k|^2$, the coefficients a_k and b_k of the states $|\Psi_0\rangle_p$ and $|\Psi_1\rangle_p$ for a 2-step DTQW, a 4-step DTQW, and a 6-step DTQW are obtained and compared with the theoretical results. Note that the error bars only indicate statistical uncertainty, which are obtained by numerical simulations. Our results indicate that the protocol introduced here is realizable in experiments and DTQW with small errors can be implemented by using the setup shown in Fig. 2.

Since the walker is initially in a superposition state of positions $| -1\rangle_p$ and $|1\rangle_p$, the outermost positions of the walker after an n -step DTQW are denoted by $| -n-1\rangle_p$ and $|n+1\rangle_p$. To simplify the calculation of a_k and b_k , we have used $a_{n+1} = 0$ and $b_{-n-1} = 0$ for this type of DTQW. In this case, only n different $\Delta\theta$ are needed to obtain a_k and b_k for an n -step DTQW.

The initial state of the walker's position can be easily prepared by rotating the angles of the HWPs in our experiment. We have also experimentally studied the DTQW with the initial state $(0.6| -2\rangle_p + |0\rangle_p + 0.8|2\rangle_p)|0\rangle / \sqrt{2}$. The results of the reconstructed a_k , b_k and $|a_k|^2 + |b_k|^2$ after 6-step DTQW are shown in Fig. 4, which also fit well with the theoretical results.

By means of this DTQW experiment, we also study the relation between the spread speed s and the initial state of the walker's position. The spread speed s is defined as $s(n) = [\sigma(n) - \sigma(0)]/n$, where $\sigma(n)$ is the variance of the position for an n -step DTQW. The results for a 4-step DTQW are obtained and plotted in Fig. 5(a), in which the

initial state is set as $(\alpha| -1\rangle_p + \sqrt{1 - \alpha^2}|1\rangle_p)(|0\rangle + i|1\rangle)/\sqrt{2}$, with $\alpha \in (-1, 1)$. It is shown that different initial states of the walker's position will lead to different spread speeds of DTQW. Especially, for the DTQWs with α and $-\alpha$ ($\alpha \neq 0$), they have different $\sigma(n)$ and $s(n)$ ($n > 0$) though starting with the same $\sigma(0)$, which is quite different from the classical random walk as shown in Fig. 5(a), because of the quantum interference.

In Fig. 5(a), we also give the simulated relation of $s \sim \alpha$ for a 16-step and 50-step DTQW. It is shown that the properties of the DTQW starting from superposition states of walker are very different from that starting from a single position of walker. For example, the parameter s for $\alpha \neq 0$ approaches a constant more slowly than that for $\alpha = 0$ as the number of DTQW steps increases.

A significant advantage of our DTQW protocol is that the whole final state (and the density matrix) of the coin and the walker's position can be obtained, rather than the position distributions only in other DTQW experimental schemes. In this case, we can investigate the entanglement between the coin and the walker in experiments by calculating the entropy of the reduced density matrix of the coin. The entropy is defined as $E = -\text{Tr}(\rho_c \ln \rho_c)$, where $\rho_c = \text{Tr}_x(\rho_{cx})$ is obtained by tracing out the walker's position. In Fig. 5(b), a relation between the entropy E and the walker's initial state from the experiment is compared with the theoretical results for 4-step DTQW. The initial states used here are the same as that for Fig. 5(a), whose entropies are 0. We show that different initial states of the walker will lead to different entropies after DTQW steps. The results for 16-step and 50-step DTQW are also plotted in Fig. 5(b). As the number of DTQW steps increases, the entropy will approach a constant value rapidly for all α , not only for $\alpha = 0$ [34]. Comparing Fig. 5(a) with Fig. 5(b), it is clear that in general a larger spread speed of DTQW corresponds to a larger entanglement between the coin and the walker.

III. DISCUSSION

To implement DTQW for larger steps, the errors of the experiment should be analyzed and improved. The errors are related to the following factors:

(i) **The number of coincidence counts.** Because of the leakage of photons at BS 1, the number of coincidence counts will decrease rapidly with increasing the DTQW steps. The ratio of reflection to transmission of all beam splitters adopted in our experiment is 50:50. The loss of detected photons after every two steps of DTQW is about 70%. It is an advantage of two optical loops adopted in the setup: photons are leaked and detected after every two steps rather than after each step.

The errors in the experiment can be reduced by increasing the number of coincident counts. One method is to replace the 50:50 coupler (i.e., BS 1) by a coupler with better ratios. The other method is to increase the number of input photons. This can be achieved in several ways. For example, the BBO can be replaced by a high-efficiency periodically poled KTiOPO4 (PPKTP), the power of the laser can be improved, or weak laser pulses can be directly used as the input photons of DTQW.

(ii) **The quality of the interference in the optical loops.** Quantum walks are different from classical random walks because of quantum interference. There are two optical loops in the setup. To guarantee good interference of DTQW, optical paths of anticlockwise and clockwise must be adjusted to be the same in each loop and two loops must be adjusted to match each other. In general, the quality of the interference will become worse when increasing walk steps. An important factor leading to interference degradation is the imperfections of devices, such as the reflection-dependence of the polarization and nonplanar optical surfaces [31, 32].

To show the scalability of this DTQW protocol and the setup, we estimate the maximum number of steps that are in principle achievable. We assume the use of perfect devices (including detectors). In addition, we assume that the loss of detected photons after every two steps of DTQW is 70%. By replacing the 50:50 coupler with a 99:1 coupler and replacing the input single photons with laser pulses of 1.4 W power (5 MHz), there should be $\sim 10,000$ photons detected in one second after 150 steps, provided that the signal-to-noise ratio can be improved by adding an active switch to couple the photons out of the loops.

In summary, we have experimentally demonstrated a 1D DTQW with the walker moving in the polarization space of single photons. This work differs from previous works in that the walker is initially in a superposition state and the walker's position is encoded using the photon polarization state. The ability to operate with arbitrary initial superposition states of DTQW and to implement DTQWs in a low-dimensional space opens an avenue for not only discovering more properties of DTQWs but also more DTQW applications. This DTQW protocol is quite general and can be applied to other quantum systems (e.g., cavity or circuit QED systems). This work may be extended to realize multi-dimensional DTQW, which is of importance for large-scale quantum computing based on quantum walks. Moreover, the proposed encoding method enables one to encode an arbitrary high-dimensional quantum state using a single physical qubit and may be adopted to implement other quantum information tasks.

IV. METHODS

The encoding method

Suppose there is an n -dimensional state

$$|\Psi\rangle = \sum_{k=1}^n a_k |k\rangle \quad \text{with} \quad \sum_{k=1}^n |a_k|^2 = 1, \quad (3)$$

in which $|k\rangle$ ($k = 1, 2, \dots, n$) are orthogonal states. In the following, we propose a method to encode this state with a two-dimensional qubit and to read out all a_k from the qubit by measurement. The obtained a_k can be used to reconstruct the n -dimensional state $|\Psi\rangle$ of Eq. (3).

The state $|\Psi\rangle$ can be encoded by using n non-orthogonal states $|k\rangle_q = \cos\theta_k|0\rangle + e^{i\phi_k}\sin\theta_k|1\rangle$ ($k = 1, 2, \dots, n$) of a qubit, which correspond to n different points in the Bloch sphere of the qubit. With $|k\rangle$ replaced by $|k\rangle_q$, the state of the qubit in the encoded state can be expressed as

$$|\Psi\rangle_q = \frac{1}{N_q} \sum_{k=1}^n a_k |k\rangle_q = \frac{1}{N_q} (C_0|0\rangle + C_1|1\rangle), \quad (4)$$

where $C_0 = \sum_{k=1}^n a_k \cos\theta_k$, $C_1 = \sum_{k=1}^n a_k e^{i\phi_k} \sin\theta_k$, and $N_q = \sqrt{|C_0|^2 + |C_1|^2}$. Note that the same state $|\Psi\rangle_q$ can be constructed by performing suitable operations on an initial state of the qubit, which is just the case considered in the DTQW protocol below.

We now show how to read out a_k from $|\Psi\rangle_q$. The density matrix of the encoded state $|\Psi\rangle_q$ can be expressed as

$$\rho_q = \frac{1}{N_q^2} \begin{pmatrix} C_0^* C_0 & C_1^* C_0 \\ C_0^* C_1 & C_1^* C_1 \end{pmatrix}, \quad (5)$$

which can be easily obtained by using tomographic measurement on the qubit. Then one homogeneous equation of a_k can be obtained as

$$C_0 - R \cdot C_1 = 0 \Rightarrow \sum_{k=1}^n (\cos\theta_k - R \cdot e^{i\phi_k} \sin\theta_k) \cdot a_k = 0, \quad (6)$$

where $R = C_0/C_1$ is obtained from the measured ρ_q as

$$R = \rho_{q11}/\rho_{q21} = \rho_{q12}/\rho_{q22}. \quad (7)$$

In this way, $n - 1$ homogeneous equations for a_k can be obtained by repeatedly encoding the state $|\Psi\rangle$ onto a qubit with $n - 1$ different sets $\{|1\rangle_q^j, |2\rangle_q^j, \dots, |n\rangle_q^j\}$ (where $j = 1, 2, \dots, n - 1$, and $|k\rangle_q^j = \cos\theta_k^j|0\rangle + e^{i\phi_k^j}\sin\theta_k^j|1\rangle$), and by measuring the corresponding R^j one at a time. Then a_k ($k = 1, \dots, n$) can be solved from the $n - 1$ homogeneous equations

$$\sum_{k=1}^n (\cos\theta_k^j - R^j \cdot e^{i\phi_k^j} \sin\theta_k^j) \cdot a_k = 0 \quad (8)$$

and the normalization condition $\sum_{k=1}^n |a_k|^2 = 1$. Now the n -dimensional encoded state is reconstructed.

To exhibit the generality and scalability of this encoding method, we calculated the fidelity between random 50-dimensional encoded states and their reconstructed states from numerical simulations of the encoding process, in which random errors of measured R^j were assumed to be within $\pm 10\%$ and a specific choice of the non-orthogonal states

$$|k\rangle_q^j = \cos(jk\Delta\theta)|0\rangle + e^{ik\Delta\phi}\sin(jk\Delta\theta)|1\rangle \quad (9)$$

was used (i.e., $\theta_k^j = jk\Delta\theta$ and $\phi_k^j = k\Delta\phi$). The averaged fidelity over 1000 random simulations is obtained and its dependence on $\Delta\theta$ and $\Delta\phi$ is plotted in Fig. 6(a). The averaged fidelity is larger than 90% in the $\sim 41\%$ area of $\Delta\theta \in (0, 180^\circ)$ and $\Delta\phi \in (0, 360^\circ)$. It is not hard to find suitable θ_k and ϕ_k to implement the encoding method, and high fidelity can be achieved for encoding large dimensional states if measurement errors are not very large.

Moreover, we experimentally demonstrated the encoding and reading of a 16-dimensional state in linear optics system. At first, we encode a uniform state $\Phi_{16} = \frac{1}{4} \sum_{k=1}^{16} |k\rangle$ in the 2-dimensional polarization space of single

photons by using $\Delta\theta = 22^\circ$ and $\Delta\phi = 12^\circ$ in Eq. (9). This encoding can be easily implemented by injecting photons into an adjusted setup consisting of two QWPs and one HWP, which can be used to construct an arbitrary one-qubit gate in the polarization space. Then density matrixes of the encoding photons can be measured and the initial uniform state can be reconstructed. The experimental result of the reconstructed state is shown in Fig. 6(b), and a high fidelity of 99.1% is achieved.

The encoding method introduced here is feasible for the present technology of linear optics and can be easily applied in other quantum systems. One key advantage for the use of this encoding method is the simplicity of setup, because only one physical qubit is needed.

ACKNOWLEDGMENTS

This work is supported in part by the NKRDP of China (Grant No. 2016YFA0301802) and the National Natural Science Foundation of China under Grant Nos [11504075, 11374083, 11774076, 11375003, 11775065]. This work is partially supported by the MURI Center for Dynamic Magneto-Optics via the AFOSR Award No. FA9550-14-1-0040, the Army Research Office (ARO) under grant number 73315PH, the AOARD grant No. FA2386-18-1-4045, the IMPACT program of JST, CREST Grant No. JPMJCR1676, JSPS-RFBR Grant No. 17-52-50023.

CONFLICT OF INTERESTS

The authors declare that they have no conflict of interest.

CONTRIBUTIONS

Q.P.Su devised various aspects of the project and designed the experimental methodology. Q.P.Su, Y.Zhang, J.Q.Zhou and S.J.Xiong carried out the experiment and analyzed the data. Q.P.Su, L.Yu, C.P.Yang, J.S.Jin and X.Q.Xu developed the theoretical aspects. Q.P.Su, C.P.Yang and F.Nori wrote the manuscript, with contributions from K.F.Chen, Z.Sun and Q.J.Xu. All authors discussed the results and contributed to refining the manuscript.

-
- [1] Aharonov, Y., Davidovich, L. & Zagury, N. Quantum random walks. *Phy. Rev. A* 48, 1687 (1993).
 - [2] Shenvi, N., Kempe, J. & BirgittaWhaley, K. Quantum random-walk search algorithm. *Phys. Rev. A* 67, 052307 (2003).
 - [3] DiFranco, C., McGettrick, M. & Busch, T. Mimicking the probability distribution of a two-dimensional Grover walk with a single-qubit coin. *Phys. Rev. Lett.* 106, 080502 (2011).
 - [4] Jeong, Y.-C., Franco, C. D., Lim, H.-T., Kim, M. S. & Kim, Y.-H. Experimental realization of a delayed-choice quantum walk. *Nat. Comm.* 4, 2471, (2013).
 - [5] Crespi, A. et al. Anderson localization of entangled photons in an integrated quantum walk. *Nat. Photon.* 7, 322 (2013).
 - [6] Zhan, X. et al. Detecting Topological Invariants in Nonunitary Discrete-Time Quantum Walks. *Phys. Rev. Lett.* 119, 130501 (2017).
 - [7] Peruzzo, A. et al. Quantum walks of correlated photons. *Science* 329, 1500 (2010).
 - [8] Kitagawa, T., Rudner, M. S., Berg, E. & Demler, E. Exploring topological phases with quantum walks. *Phys. Rev. A* 82, 033429 (2010).
 - [9] Buluta, I. & Nori, F. Quantum simulators. *Science* 326, 5949 (2009).
 - [10] Georgescu, I. M., Ashhab, S. & Nori, F. Quantum simulation. *Rev. Mod. Phys.* 86, 153 (2014).
 - [11] Childs, A. M. Universal computation by quantum walk. *Phys. Rev. Lett.* 102, 180501 (2009).
 - [12] Underwood, M. S. & Feder, D. L. Universal quantum computation by discontinuous quantum walk. *Phys. Rev. A* 82, 042304 (2010).
 - [13] Childs, A. M., Gosset, D. & Webb, Z. Universal computation by multiparticle quantum walk. *Science* 339, 791 (2013).
 - [14] Kurzynski, P. & Wojcik, A. Quantum walk as a generalized measuring device. *Phys. Rev. Lett.* 110, 200404 (2013).
 - [15] Reberntrost, P., Mohseni, M., Kassar, I., Lloyd, S. & Guzik, A. A. Environment-assisted quantum transport. *New J. Phys.* 11, 033003 (2009).
 - [16] Kempe, J. Quantum random walks: an introductory overview. *Conte. Phys.* 44, 307 (2003).
 - [17] Venegas-Andraca, S. E. Quantum walks: a comprehensive review. *Quan. Inf. Proc.* 11, 1015 (2012).
 - [18] Strauch, F. W. Relativistic quantum walks. *Phys. Rev. A* 73, 054302 (2006)

- [19] Chandrashekar, C. M. & Laflamme, R. Quantum phase transition using quantum walks in an optical lattice. *Phys. Rev. A* 78, 022314 (2008)
- [20] Romanelli, A. Distribution of chirality in the quantum walk: Markov process and entanglement. *Phys. Rev. A* 81, 062349 (2010)
- [21] Valcuel, G. J., Roldn, E. & Romanelli, A. Tailoring discrete quantum walk dynamics via extended initial conditions. *New J. Phys.* 12, 123022 (2010)
- [22] Zhang, W. W., Goyal, S. K., Gao, F., Sanders, B. C. & Simon, C. Creating cat states in one-dimensional quantum walks using delocalized initial states. *New J. Phys.* 18, 093025 (2016)
- [23] Xue, P. et al. Experimental quantum-walk revival with a time-dependent coin. *Phys. Rev. Lett.* 114, 140502 (2015).
- [24] Do, B. et al. Experimental realization of a quantum quincunx by use of linear optical elements. *Opt. Soc. Am. B* 22, 020499 (2005).
- [25] Sansoni, L. et al. Two-particle bosonic-fermionic quantum walk via integrated photonics. *Phys. Rev. Lett.* 108, 010502 (2012).
- [26] Xue, P. & B. C. Sanders Two quantum walkers sharing coins. *Phys. Rev. A* 85, 022307 (2012).
- [27] Schmitz, H. et al. Quantum walk of a trapped ion in phase space. *Phys. Rev. Lett.* 103, 090504 (2009).
- [28] Zahringer, F. et al. Realization of a quantum walk with one and two trapped ions. *Phys. Rev. Lett.* 104, 100503 (2010).
- [29] Flurin, E. et al. Observing Topological Invariants Using Quantum Walks in Superconducting Circuits. *Phys. Rev. X* 7, 031023 (2017).
- [30] Karski, M. et al. Quantum walk in position space with single optically trapped atoms. *Science* 325, 174 (2009).
- [31] Broome, M.A. et al. Discrete single-photon quantum walks with tunable decoherence. *Phys. Rev. Lett.* 104, 153602 (2010).
- [32] Schreiber, A. et al. Photons walking the line: a quantum walk with adjustable coin operations. *Phys. Rev. Lett.* 104, 050502 (2010).
- [33] Bouwmeester, D., Marzoli, I., Karman, G.P., Schleich, W. & Woerdman, J.P. Optical galton board. *Phys. Rev. A* 61, 013410 (1999).
- [34] Carneiro, I. et al. Entanglement in coined quantum walks on regular graphs. *New J. Phys.* 7, 156 (2005).

FIGURE LEGENDS

Fig. 1

(a) Encoding of the walker's position and the implementation of conditional translation T_p in the polarization space. $|H\rangle$ ($|V\rangle$) is the horizontal (vertical) polarization state. (b) Optical realization of the time-independent evolution operator $U = T_p S_c$ for DTQW, in which the coin is tossed by the beam splitter (BS) and the conditional transition of the walker's positions $|k\rangle_p$ is implemented by two half-wave plates (HWPs) oriented at $\Delta\theta/2$ (for the coin state $|0\rangle$) and $-\Delta\theta/2$ (for the coin state $|1\rangle$) and two 0° HWPs.

Fig. 2

Schematic of the experimental setup for quantum walk in the polarization space, in which D_0 is a single-photon detector and D_1 (D_2) represents the standard polarization analysis detector. A pair of photons are generated in the BBO crystal. One photon is detected directly by D_0 as the trigger and another photon is adopted to make the DTQW. The initial states of the coin and the walker are prepared in the light yellow block. The DTQW is realized with two optical loops. The photons experience different steps of DTQW and can be distinguished by their arrival times at D_1 or D_2 after a trigger event. PBS: polarizing beam splitter.

Fig. 3

Theoretical and experimental results of the 1D Hadamard DTQW after 2, 4, and 6 steps with an initial state of $(0.8|-1\rangle_p + 0.6|1\rangle_p)|0\rangle$. The green (blue) bars represent the experimental (theoretical) results. The red error bars represent statistical errors.

Fig. 4

Theoretical and experimental results for the 6-step DTQW with an initial state of $(0.6|-2\rangle_p + |0\rangle_p + 0.8|2\rangle_p)|0\rangle/\sqrt{2}$. The green (blue) bars show the experimental (theoretical) results. The red error bars represent statistical errors.

Fig. 5

(a) Relation between the spread speed s and the initial state of the walker's position for 4-step (red), 16-step (blue) and 50-step (green) DTQW. The thin solid curves are from the corresponding classical random walks for 4, 16, and 50 steps, which have a symmetry on the two sides of $\alpha = 0$. (b) Relation between the entropy E and the initial state of the walker's position for 4-step (red), 16-step (blue) and 50-step (green) DTQW. The initial state of the DTQW is assumed as $(\alpha|-1\rangle_p + \sqrt{1-\alpha^2}|1\rangle_p)(|0\rangle + i|1\rangle)/\sqrt{2}$. The curves are from our theoretical calculations. The red dots show the experimental data and the red error bars represent statistical errors.

Fig. 6

(a) Numerical simulations for the fidelity of the encoding of 50-dimensional states into qubits. (b) Experimental results for the reconstruction of a 16-dimensional state $\frac{1}{4}\sum_{k=1}^{16}|k\rangle$ from encoded single photons in a linear-optical system.

FIGURES

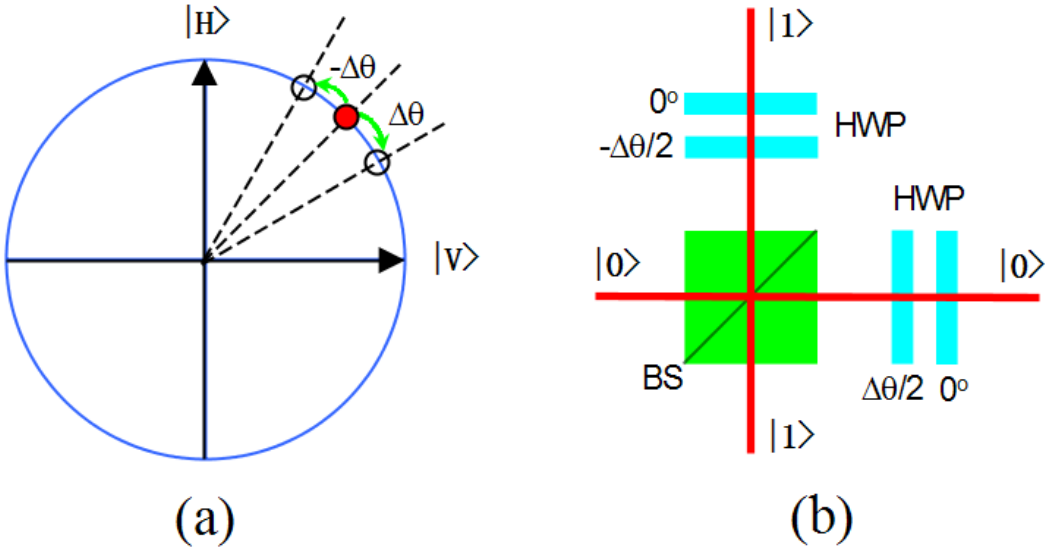


FIG. 1.

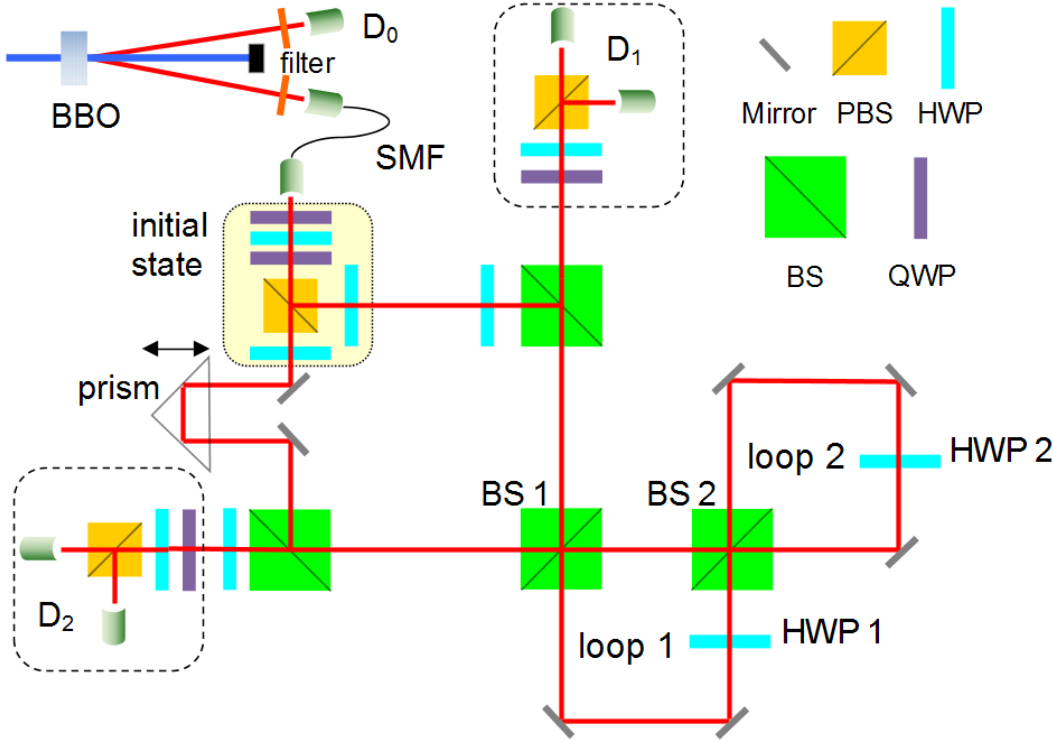


FIG. 2.

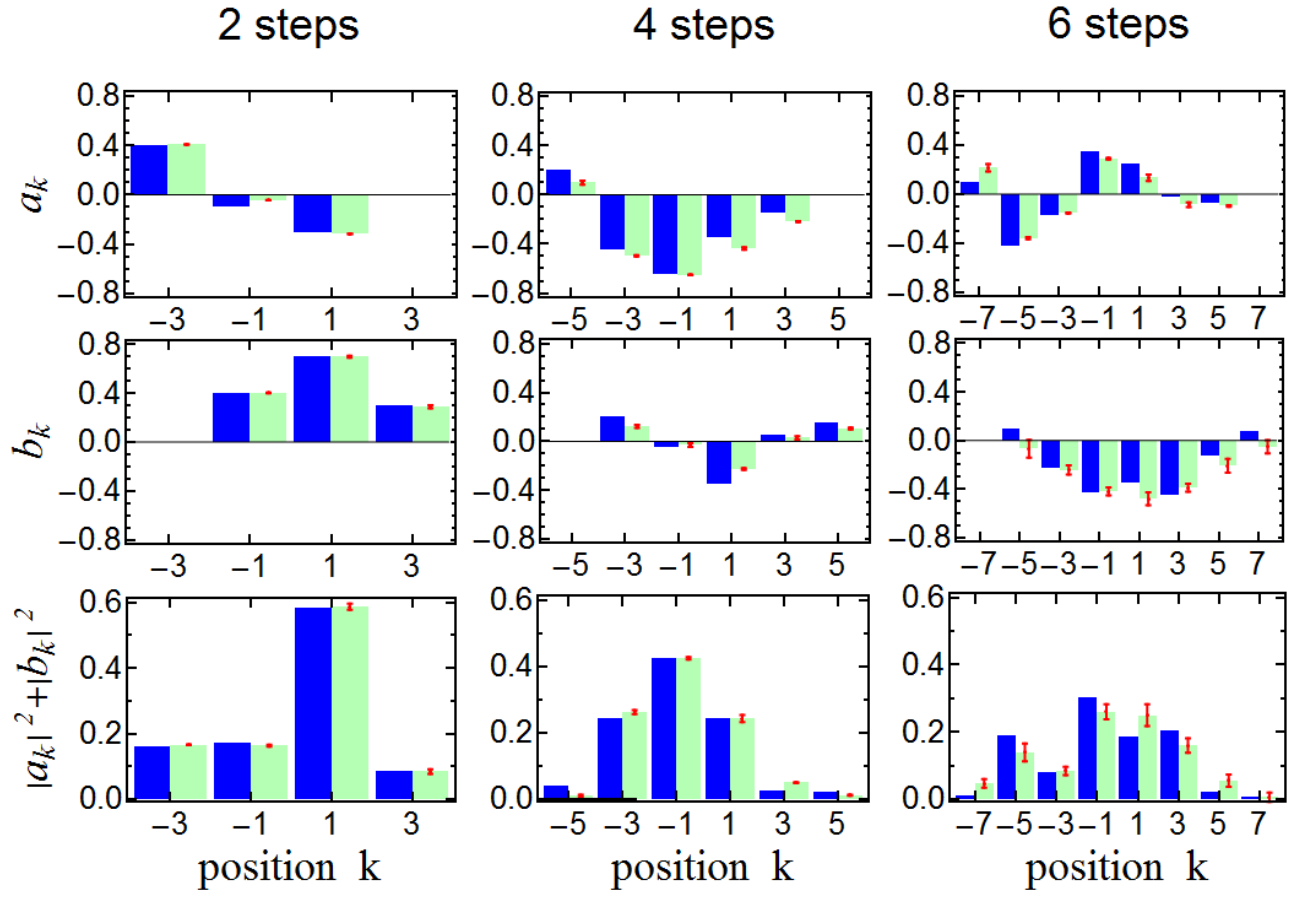


FIG. 3.

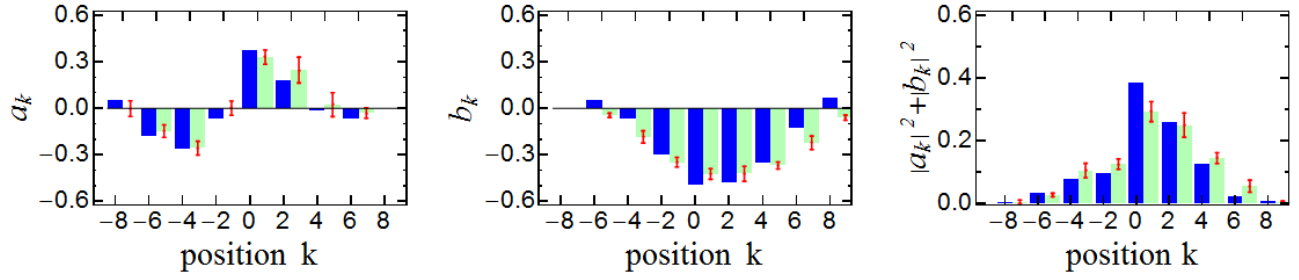


FIG. 4.

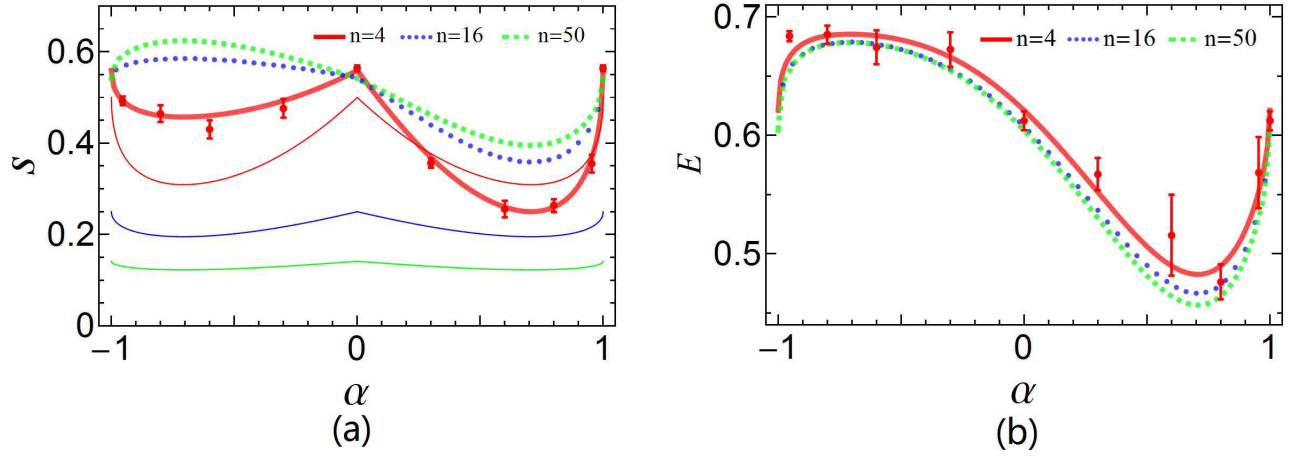


FIG. 5.

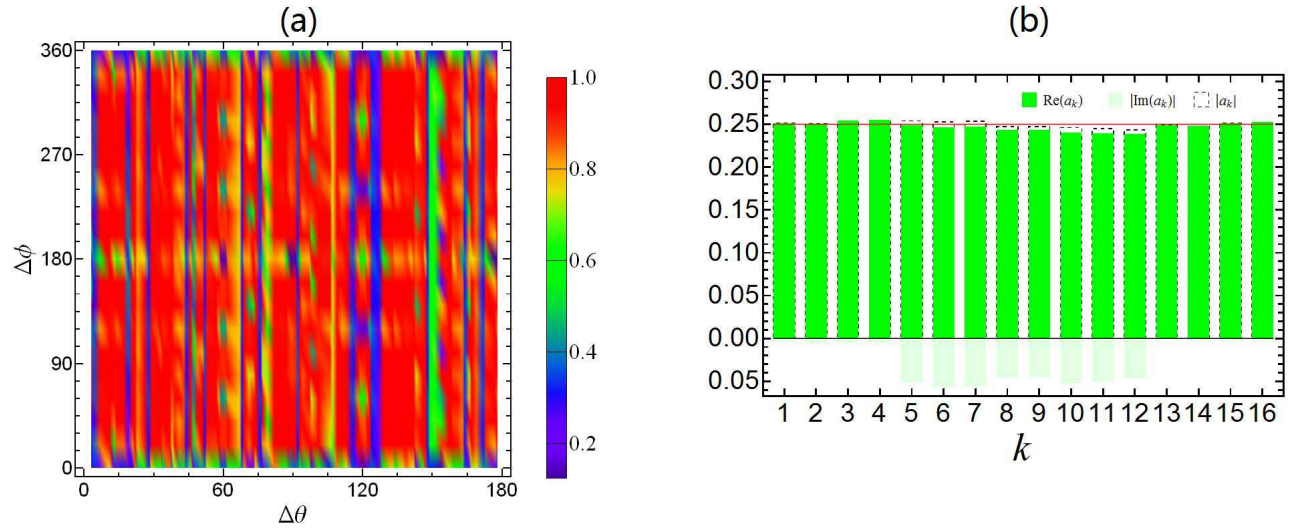


FIG. 6.